Published OnlineFirst December 28, 2016; DOI: 10.1158/1541-7786.MCR-16-0243-T

Oncogenes and Tumor Suppressors

Molecular Cancer Research

Predictive Outcomes for HER2-enriched Cancer Using Growth and Metastasis Signatures Driven By SPARC

Leandro N. Güttlein[1], Lorena G. Benedetti[1], Cristóbal Fresno[2], Raúl G. Spallanzani[3], Sabrina F. Mansilla[4], Cecilia Rotondaro[1], Ximena L. Raffo Iraolagoitia[3], Edgardo Salvatierra[1], Alicia I. Bravo[5], Elmer A. Fernández[2,7], Vanesa Gottifredi[4], Norberto W. Zwirner[3,6], Andrea S. Llera[1], and Osvaldo L. Podhajcer[1]

Abstract

Understanding the mechanism of metastatic dissemination is crucial for the rational design of novel therapeutics. The secreted protein acidic and rich in cysteine (SPARC) is a matricellular glycoprotein which has been extensively associated with human breast cancer aggressiveness although the underlying mechanisms are still unclear. Here, shRNA-mediated SPARC knockdown greatly reduced primary tumor growth and completely abolished lung colonization of murine 4T1 and LM3 breast malignant cells implanted in syngeneic BALB/c mice. A comprehensive study including global transcriptomic analysis followed by biological validations confirmed that SPARC induces primary tumor growth by enhancing cell cycle and by promoting a COX-2–mediated expansion of myeloid-derived suppressor cells (MDSC). The role of SPARC in metastasis involved a COX-2–independent enhancement of cell disengagement from the primary tumor and adherence to the lungs that fostered metastasis implantation. Interestingly, SPARC-driven gene expression signatures obtained from these murine models predicted the clinical outcome of patients with HER2-enriched breast cancer subtypes. In total, the results reveal that SPARC and its downstream effectors are attractive targets for antimetastatic therapies in breast cancer.

Implications: These findings shed light on the prometastatic role of SPARC, a key protein expressed by breast cancer cells and surrounding stroma, with important consequences for disease outcome. *Mol Cancer Res; 15(3); 304–16. ©2016 AACR.*

Introduction

Breast cancer is the second cause of cancer-related death among women in most countries. Only 25% of the patients with metastatic disease survive after 5 years (1). Global transcriptomic analysis of primary breast cancer samples has shown the existence of a molecular signature predictive of metastatic development embedded in the primary tumor (2) indicating that the cell clones responsible for cancer dissemination are already present in the primary tumor.

Previous studies performed in women who died of metastatic breast cancer showed that more than 80% of metastasis deposits were in the lungs and pleura (3). SPARC has been heralded as one of the very few genes that acts in a concerted way to promote the establishment of lung metastasis (4). SPARC expression in breast cancer was associated with the less differentiated grade 3 samples (5) and with the more aggressive $CD44^{+}$ basal-like samples (6). SPARC was proposed as an independent marker of poor prognosis for *in situ* ductal carcinoma (7), invasive ductal carcinoma (8), and breast cancer as a whole (9). mRNA sequencing studies identified SPARC as one of the top 6 transcripts in breast cancer primary tumor samples (10). *In silico* analysis associated SPARC expression with poor prognosis in patients with HER2-enriched breast cancer (11). While most studies associated SPARC expression with the more aggressive forms of breast cancer and with poor prognosis, other studies seem to contradict this view. The expression of SPARC in combination with TIMP3, FN1, and LOX was significantly associated with distant metastasis-free survival in lymph node–negative patients (12). Additional studies showed that strong expression of stromal cell–derived SPARC in breast cancer samples appear to correlate with survival (13). In addition, low SPARC staining has been shown to correlate with poor prognosis in patients with luminal A or triple-negative breast cancer (TNBC; ref. 14).

[1]Laboratorio de Terapia Molecular y Celular, IIBBA, Fundación Instituto Leloir, CONICET, Buenos Aires, Argentina. [2]Unidad Asociada: Área de Cs. Agrarias, Ingeniería, Cs. Biológicas y de la Salud. CONICET. Universidad Católica de Córdoba, Córdoba, Argentina. [3]Laboratorio de Fisiopatología de la Inmunidad Innata, Instituto de Biología y Medicina Experimental-CONICET. Buenos Aires, Argentina. [4]Laboratorio de Ciclo Celular y Estabilidad Genómica, IIBBA, Fundación Instituto Leloir, CONICET, Buenos Aires, Argentina. [5]Unidad de Inmunopatología, Hospital Interzonal General de Agudos Eva Perón, San Martín, Provincia de Buenos Aires, Argentina. [6]Facultad de Ciencias Exactas y Naturales, Departamento de Química Biológica, Universidad de Buenos Aires, Buenos Aires, Argentina. [7]Facultad de Ciencias Exactas, Físicas y Naturales, Universidad Nacional de Córdoba, Córdoba, Argentina.

Note: Supplementary data for this article are available at Molecular Cancer Research Online (http://mcr.aacrjournals.org/).

L.N. Güttlein and L.G. Benedetti contributed equally to this article.

A.S. Llera and O.L. Podhajcer are co-senior authors of this article.

Corresponding Author: Osvaldo L. Podhajcer, IIBBA, Fundacion Instituto Leloir, CONICET, Av. Patricias Argentinas 435, Buenos Aires C1405BWE, Argentina. Phone: 5411-5238-7500; Fax: 5411-5238-7501; E-mail: opodhajcer@leloir.org.ar

doi: 10.1158/1541-7786.MCR-16-0243-T

Published OnlineFirst December 28, 2016; DOI: 10.1158/1541-7786.MCR-16-0243-T

This controversy was also observed in *in vitro* and *in vivo* studies using murine models. SPARC has been identified as one of the four genes that promotes lung metastasis (4) and its expression in MCF-7 cells promoted epithelial–mesenchymal transition (EMT), through Snail (15). Knockdown of its expression in MCF7 cells impaired motility and invasive capabilities (16). Moreover, breast cancer cells respond to SPARC by showing increased activity of MMP-2, a potential mechanism that might facilitate cell dissemination (17). On the contrary, enforced overexpression of SPARC in MDA-MB-231 cells diminished bone metastases through the reduction of tumor cell–platelet aggregation (18).

Using immunocompromised mice models, it was shown that knockdown of SPARC expression in human melanoma cells induced tumor rejection by an IL8/GRO–driven recruitment and activation of polymorphonuclear cells (19, 20). SPARC-producing mammary carcinoma cells exhibited a reduced tumor growth in SPARC-null mice and an increased infiltration of $CD45^+$ leucocytes compared with wild-type mice (21). Moreover, SPARC expressed by tumor-infiltrating macrophages increased the dissemination of 4T1 mammary cancer cells in a SPARC-null mice model (22). These reports suggest a link between SPARC and the inflammatory response that cannot be fully assessed in immunocompromised models. Here, we performed a comprehensive study in immunocompetent mice models aimed to clarify the role of SPARC in breast cancer progression and identify downstream mechanisms and effectors. By knocking down SPARC expression in malignant breast cancer cells, we show that SPARC promotes primary tumor growth and dissemination through downstream effectors that affect cell cycling/viability, immune response, and extracellular matrix remodeling. A SPARC-dependent molecular signature derived from these studies was able to identify patients with worse prognosis in the HER2-enriched human breast cancer subtype.

Materials and Methods

Mice and human samples

Female BALB/c mice (6–8 weeks) were housed at the animal facility of Leloir Institute (NIH A5168-01). All the *in vivo* experiments were approved by the Institutional Animal Care and Use Committee (IACUC-FIL, Protocols 51 and 69). Paraffin-embedded tumor sections were obtained from the Service of Pathology, Eva Peron Hospital, San Martín, Buenos Aires, Argentina following institutional guidelines (Supplementary Table S1).

Cell culture

Authenticated 4T1 and MCF7 cells were purchased from the ATCC between 2009 and 2011. LM3 cells were kindly provided by Elisa Bal (Institute of Oncology "Angel H. Roffo", University of Buenos Aires, Aires, Argentina). All the cell lines were grown in the recommended media, supplemented with 10% FBS (Natocor) and antibiotics, and maintained at 37°C, 5% CO_2 for no longer than 5 passages. To generate spheroids, dispersed cells were seeded in 96-well plates precoated with 75 μL of 1% agarose at a density of 1×10^4 cells per well. All the cells were routinely tested for mycoplasma contamination by PCR (23). Stable knockdown of SPARC and stable expression of COX-2 and SPARC was carried out as described in the Supplementary Materials and Methods.

In vivo assays

A total of 2×10^5 cells were subcutaneously injected in the mammary fat pad of BALB/c mice in 50 μL of serum-free PBS. Tumor volume was calculated as $V = d_s^2 d_l/2$, where d_s and d_l are the smaller and larger diameters, respectively. When mice showed physiologic signs of distress (i.e., piloerection and respiratory failure), they were euthanized and tumors were removed and fixed in 10% buffered formalin for immunohistochemical studies. Metastasis foci were counted after fixing lungs with 10% buffered formalin. For quantification of circulating tumor cells, tumor-bearing mice were bled from the submandibular region 7 and 14 days after cell injection. Erythrocytes were lysed with buffered ammonium chloride solution (ACK buffer) for 5 minutes and the remaining cells were resuspended in selective media with G418 (Invitrogen) and cultured for 4 weeks in 10-cm tissue culture plates. Images were captured under ×100 magnification and clonogenic GFP^+ colonies were counted with a CellProfiler homemade pipeline (24). For the analysis of lung adhesion capability, 1×10^5 4T1 cells prestained with DiR (Molecular Probes) were intravenously injected in 0.05 mL PBS. DiR *in vivo* tracking on isolated lungs was followed with a Fluorescence Imaging (FI) IVIS Lumina Bioluminometer (Xenogen). Captured images were measured as average photons per second per square centimeter per steridian ($p/s/cm^2/sr$).

Immunohistology and immunofluorescence

After deparaffinization, 5-μm sections of human or murine samples were incubated with antibodies (Ab) against human SPARC (1:10, MAB941; R&D Systems), mouse SPARC (1:10, AF942, R&D Systems), mouse cleaved caspase-3 (1:1,000, RA15046, Neuromics), and mouse Ki67 (1:400, Cell Signaling Technology). Staining was revealed using the Vectastain Elite ABC kit (Vector Laboratories). For total collagen detection, deparaffinized sections were stained with Masson trichrome according to the standard protocols. A homemade Matlab algorithm (The Mathworks, Inc.) was used to quantify SPARC, Ki67, and collagen staining (details provided in Supplementary Materials and Methods). Cleaved caspase-3^+ cells were counted manually. COX-2 expression in murine spheroids was assessed by immunofluorescence. Briefly, spheroids were rinsed twice with PBS, fixed in 4% PFA for 1 hour, cryopreserved overnight in 30% sucrose, embedded in tissue optimum cutting temperature (OCT), and stored at −20°C. Cryostat sections of 9 μm were incubated overnight at 4°C with an anti-COX-2 Ab (1:100, ab15191, Abcam) followed by 2-hour incubation with 1/200 Cy-5–labeled donkey anti-rat Ab (Jackson Laboratories). ImageJ (25) was used to quantify spheroid fluorescence. Corrected total spheroid fluorescence (CTSF) was calculated as Integrated density − (area of selected spheroids × mean fluorescence of background). All images were captured using BX-60 Olympus fluorescent microscope.

Microarrays analysis

RNA was obtained from cells and tumors (2-day-old primary tumors and 30-day-old metastasis foci) using the RNeasy Mini Kit (Qiagen). The 2-day-old tumors could be identified as a small but palpable knob of around 1.0–1.5 mm^3 that was clearly seen on the everted skin (26). Total RNA amplification and cRNA labeling was performed using the SuperScript Indirect RNA Amplification System (Invitrogen). Profiling using the 38.5 k Murine Exonic Evidence Based Oligonucleotide (MEEBO, Microarray Inc) is

Published OnlineFirst December 28, 2016; DOI: 10.1158/1541-7786.MCR-16-0243-T

described in the Supplementary Materials and Methods. Microarray profiling data were deposited into GEO (GSE83832). mRNA levels were validated by quantitative RT-PCR as described in Supplementary Materials and Methods.

Studies with immune cells

Frequency of myeloid-derived suppressor cells (MDSC; $CD11b^+Gr\text{-}1^+$ cells) and T lymphocytes ($CD4^+$ or $CD8^+$ cells) was analyzed by flow cytometry. Briefly, cell suspensions from spleen, primary tumor, bone marrow, and lungs were labeled with mAb PE/Cy7 anti-Ly-6G/Ly-6C (Gr-1, clone RB6-8C5, Biolegend) in combination with PE/Cy5 anti-CD11b (clone M1/70, Biolegend) for MDSCs or with PeCy5 anti-CD4 (clone RM4-5 BD) or Alexa-488 anti-CD8 (clone 53-6.7, BD) for T lymphocytes subsets. Cells were analyzed on a FACSCanto II flow cytometer (BD Biosciences). $CD4^+$ and $CD8^+$ lymphocytes were depleted *in vivo* by intraperitoneal administration of 0.2 mg of mAbs against CD4 (clone YTS 191.1; ATCC) and CD8 (clone YTS 169.4; ATCC) respectively, at days −1, 1, 8, 15, and 22, relative to inoculation of malignant cells (27). Control mice received equivalent amounts of normal mouse IgG at the same days. Depletions were confirmed in peripheral blood 7 days after tumor challenge by flow cytometry using non cross-reactive Abs.

Statistical and bioinformatics analysis

Prism5 (GraphPad Software, Inc.) was used. Two groups were compared with a Student *t* test for unpaired data. ANOVA using Bonferroni posttest was used for multiple comparisons. A P value < 0.05 was considered statistically significant. Functional analysis over the Kyoto Encyclopedia of Genes and Genomes (KEGG; ref. 28) and Gene Ontology's (GO; ref. 29) biological process (BP) were performed using the different candidate gene lists for *in vivo* and *in vitro* comparisons in DAVID using the reliably detected genes for each experimental setting. Association studies between candidate genes and clinical outcome in breast cancer patients were carried out by means of survival analyses using distant metastasis–free survival (DMFS) as endpoint. See Supplementary Materials and Methods for complete description.

Other methods

Further information about the materials and methods used in this study are provided in the Supplementary Materials and Methods section.

Results

Increased SPARC expression is associated with human and murine breast cancer dissemination

Our initial studies were performed to assess whether SPARC expression in primary tumor samples from treatment-naïve patients is associated with the presence of axillary lymph node metastases. We observed that increased SPARC staining in primary tumors correlated with the presence of axillary lymph node metastases (Fig. 1A and B; Supplementary Table S1). Average SPARC intensity staining was significantly higher in primary tumors with positive axillary lymph nodes than those with no metastatic nodes (Fig. 1C). Integration of human tumor DNA microarrays and survival data from Gene Expression-Based Outcome for Breast Cancer Online tool (GOBO; ref. 30) also showed that increased SPARC mRNA level was associated with reduced DMFS only in the aggressive HER2-enriched breast cancer subtype (Fig. 1D; Supplementary Fig. S1). Taken together, these data confirmed that SPARC expression is associated with increased aggressiveness and dissemination capacity of human breast cancer.

4T1 and LM3 cells spontaneously metastasize to the lungs after implantation in the mammary fat pad of immunocompetent BALB/c mice (31, 32). Cell clones stably expressing the shRNA i52-1 targeting SPARC exhibited up to 90% decrease in SPARC mRNA and up to 80% decrease in secreted SPARC that appeared as a unique band of 43 kDa (Supplementary Fig. S2B–S2D). We confirmed no changes in the expression levels of potential off-targets of the shRNA against SPARC (Supplementary Table S3). All the 4T1- and the LM3-SPARC-deficient cell clones showed a strongly impaired capacity to grow as primary tumors (Fig. 1E; Supplementary Fig. S3A). As expected, primary tumors obtained from SPARC-deficient cell clones showed SPARC expression in stromal cells compared with 4T1-SCR control tumors that expressed SPARC both in the stromal and the malignant cells compartments (Supplementary Fig. S3B and S3C). In addition, SPARC-deficient tumors exhibited a slight but significant reduction in collagen deposition compared with control 4T1-SCR tumors (Supplementary Fig. S3D and S3E). SPARC-deficient cell clones completely lost their capacity to generate spontaneous lung metastases (Fig. 1F and G; Supplementary Fig. S3F); even when SPARC-deficient 4T1-C1 tumors were allowed to reach 1,000 mm^3, lung metastatic foci were hardly seen (Supplementary Fig. S3G and S3H). Interestingly, SPARC-deficient tumors released reduced levels of malignant cells to the circulation compared with the control tumors and these cells were unable to colonize the lung after intravenous administration (see below Fig. 6A and C). These data suggest that SPARC promotes primary tumor growth and metastatic dissemination through independent downstream mechanisms.

Transcriptomic analysis of SPARC-deficient cells and tumors revealed changes in cell cycling/viability, cell–ECM interaction, and immune response

To gain insight into the downstream effectors of SPARC, we compared the transcriptome of SPARC-deficient 4T1-C18 cells with that of 4T1-SCR control cells. Both GO and KEGG pathway analyses, using 407 differentially expressed genes (Supplementary Table S4), highlighted terms related mainly to "Cell cycle" and "cell–ECM interaction" (Fig. 2A and B; Supplementary Tables S5 and S6). Consistent with these results, SPARC-deficient cells exhibited a significantly reduced *in vitro* proliferative capacity (Fig. 2C; Supplementary Fig. S4A). Moreover, SPARC-deficient 4T1-C18 cells showed almost 16% increase in the percentage of cells in G_1 ($46\% \pm 3\%$ vs. $30\% \pm 3\%$; $P < 0{,}01$) and 9% decrease in the percentage of cells in the S-phase compared with control 4T1-SCR cells (38 ± 2 vs. 47 ± 5; $P > 0{,}05$; Fig. 2D). The lower percentage of 4T1-C18 cells in the S-phase was confirmed by bromodeoxyuridine (BrdUrd) labeling (Fig. 2E; Supplementary Fig. S4B) and by following BrdUrd staining and cell-cycle distribution analysis at different time points after hydroxyurea synchronization (Supplementary Fig. S4C and S4D). Interestingly, 4T1-C18 tumors exhibited more than 50% reduction of cycling Ki67-positive cells compared with 4T1-SCR tumors (Fig. 2F; Supplementary Fig. S4E), indicating that SPARC enhanced cell-cycle entrance also *in vivo*.

Published OnlineFirst December 28, 2016; DOI: 10.1158/1541-7786.MCR-16-0243-T

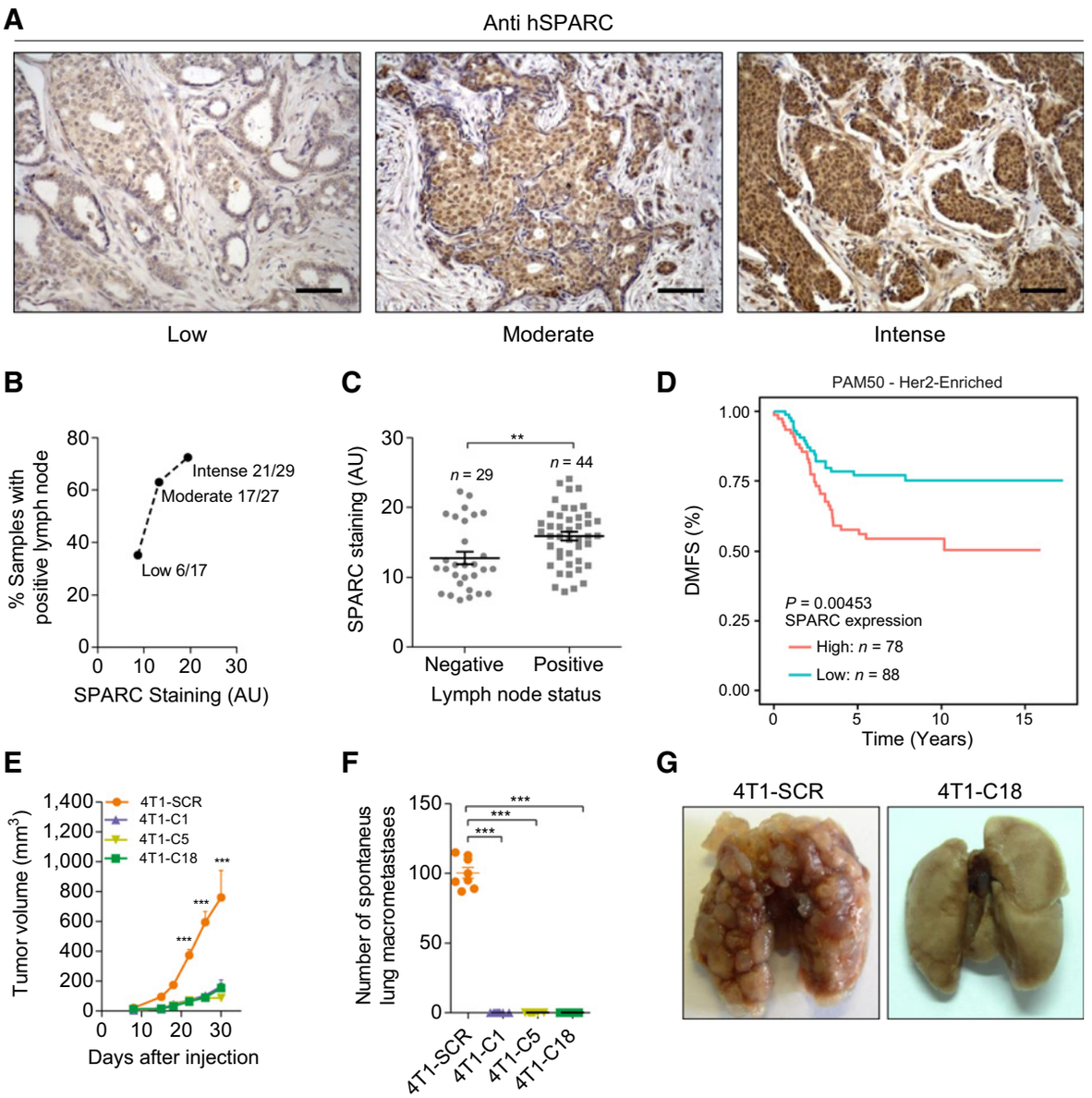

Figure 1.

SPARC expression is associated with breast cancer progression both in patients and experimental models. **A,** SPARC immunostaining of primary human breast cancer (BC) specimens ($n = 73$) classified into low ($n = 17$), moderate ($n = 27$), and intense ($n = 29$) by a pathologist (A.I. Bravo) at blind. Representative micrographs are shown. Scale bars, 100 μm. **B,** Percentage of samples with lymph node metastasis as a function of SPARC staining for each group. The fractional number of patients with positive lymph node is shown. **C,** SPARC staining in breast cancer primary tumors as a function of lymph node status. Results are expressed as mean ± SEM, **, $P < 0.01$, *t* test. **D,** Association between SPARC transcript levels and clinical outcome of breast cancer patients with HER2-enriched subtype ($n = 166$, high: 78, low: 88; $P < 0.01$). See also Supplementary Fig. S1. **E,** *In vivo* growth of SPARC-deficient 4T1 cell clones compared with control cells (4T1-SCR) in syngeneic BALB/c mice. Data are the mean ± SEM of three experiments ($n = 8$ mice per group). ***, $P < 0.001$, two-way ANOVA and Bonferroni multiple comparisons test. **F,** Quantification of spontaneous macroscopic lung foci. Results are expressed as mean ± SEM ($n = 8$ mice per group). ***, $P < 0.001$, one-way ANOVA and Bonferroni multiple comparisons test. **G,** Representative images of the experiment in **F** are shown. See also Supplementary Figs. S2 and S3.

To further identify the downstream effectors of the protumorigenic and prometastatic role of SPARC, we performed a comparative analysis of the transcriptome of 4T1-SCR primary tumors, 4T1-C18 SPARC–deficient primary tumors and 4T1-SCR metastases (4T1-SCR MTTS). For transcriptomic studies, we selected 2-day-old primary tumors (Supplementary Fig. S5A) to avoid tumor necrosis. Metastatic samples were obtained from established 30-day-old 4T1-SCR MTTS. Our previous data as well as the literature suggest the coexistence in the primary tumors of genes that promote primary tumor

Published OnlineFirst December 28, 2016; DOI: 10.1158/1541-7786.MCR-16-0243-T

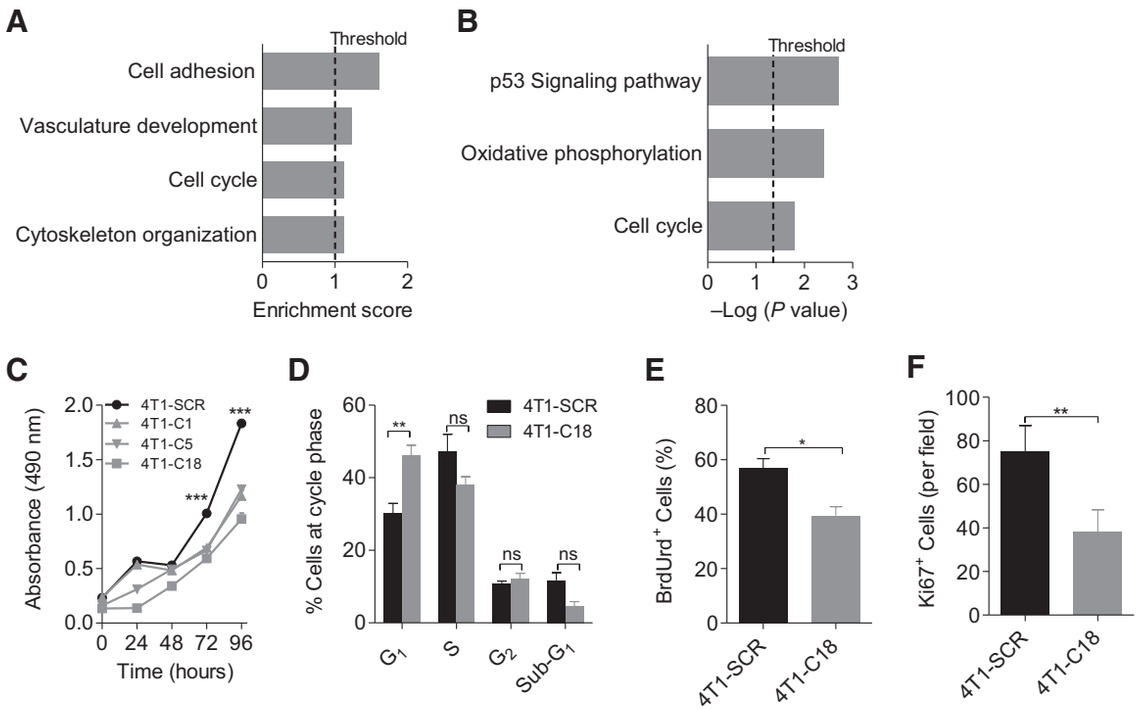

Figure 2.

SPARC modulates cell cycling. **A** and **B,** Clusters of GO Biological Process (BP) and KEGG pathway enrichment analysis of differentially expressed genes between 4T1-SCR control and SPARC-deficient 4T1-C18 cells *in vitro*. Name of clusters in **A** were arbitrary assigned according to their functionality. **C,** *In vitro* cell proliferation of the different SPARC-deficient 4T1 clones compared with control cells (4T1-SCR) analyzed by MTS assay. Data are the mean ± SEM of three experiments. ***, $P < 0.001$, two-way ANOVA and Bonferroni multiple comparisons test. **D,** Percentage of 4T1-SCR or 4T1-C18 cells in different phases of the cell cycle analyzed by flow cytometry of propidium iodide–stained cells. **E,** Percentage of cells in S-phase assessed by BrdUrd immunostaining under basal conditions. **F,** Quantification of Ki-67 staining in 4T1-SCR and 4T1-C18 tumor sections, 5 days after cells inoculation in the mammary fat pad. **E** and **F,** Data are the mean ± SEM of three experiments. ***, $P < 0.001$; **, $P < 0.01$; *, $P < 0.05$; ns, nonsignificant, *t* test. See also Supplementary Fig. S4.

(PT) outgrowth, with genes responsible for the early stages of metastasis (ESM). These genes might be under SPARC control (S-PT genes and S-ESM genes) or not (PT genes and ESM genes; Fig. 3A). A third group of genes, responsible for metastasis establishment, were not part of these analyses as SPARC-deficient cells did not establish lung metastases. On the basis of this assumption, S-PT genes correspond to the genes differentially expressed between 4T1-SCR and 4T1-C18, shared with the genes differentially expressed between 4T1-SCR and 4T1-SCR MTTS (Fig. 3B, top). Using this approach, we identified 156 S-PT genes (Supplementary Table S7; Supplementary Fig. S5B). GO and KEGG analyses revealed an enrichment in genes associated with inflammatory/immune response (Fig. 3C and D; Supplementary Tables S8 and S9). Technical validation of 9 S-PT genes by qPCR confirmed the downregulation of proinflammatory genes, like *Il6*, GRO-α (*Cxcl1*), and cyclooxygenase-2 (*Ptgs2*), in SPARC-deficient 4T1-C18 tumors compared with 4T1-SCR tumors (Fig. 3E). The expression of these proinflammatory genes is also downregulated in lung foci compared with the 4T1-SCR primary tumor (Supplementary Table S7).

On the other hand, S-ESM genes are among those differentially expressed between 4T1-SCR and 4T1-C18 and shared with the genes differentially expressed between 4T1-C18 and 4T1-SCR MTTS (Fig. 3B, bottom; Supplementary Table S10; Supplementary Fig. S5C). GO and KEGG analysis of the 165 S-ESM genes showed enrichment in terms related with ECM organization (Fig. 3E; Supplementary Table S11) and "ECM–receptor interaction", respectively (Fig. 3F; Supplementary Table S12). We technically validated by qPCR the expression levels of S-ESM genes widely associated with cell–ECM interaction, such as fibronectin 1 (*Fn1*), osteopontin (*Spp1*), and collagen 6 (alpha1) (*Col6a1*; Fig. 3G) among others. Thus, SPARC-driven cell–ECM interaction appears to play a key role in breast cancer dissemination and colonization of the lungs.

Expression of COX-2 in SPARC-deficient cells restores primary tumor growth but not the metastatic capacity

From the previous analysis, COX-2 seems to be a candidate to validate the existence of S-PT genes. Initially, we observed no correlation between SPARC and COX-2 levels in cells growing in two-dimensional layers (Fig. 4A). As the *in vivo* transcriptome study was performed on 2-day-old tumors, we hypothesized that the *in vivo* changes occur very early and might be related to the tumor architecture rather than the tumor–stroma interaction. To mimic this scenario, we prepared spheroids and observed a dramatic decrease in COX-2 levels in SPARC-deficient spheroids compared with 4T1-SCR spheroids (Fig. 4B and C). COX-2 expression in 4T1-C18 spheroids was rescued upon exogenous SPARC addition (Fig. 4C and D). Moreover, enforced expression of SPARC in MCF7 spheroids also induced a dramatic increase in

Published OnlineFirst December 28, 2016; DOI: 10.1158/1541-7786.MCR-16-0243-T

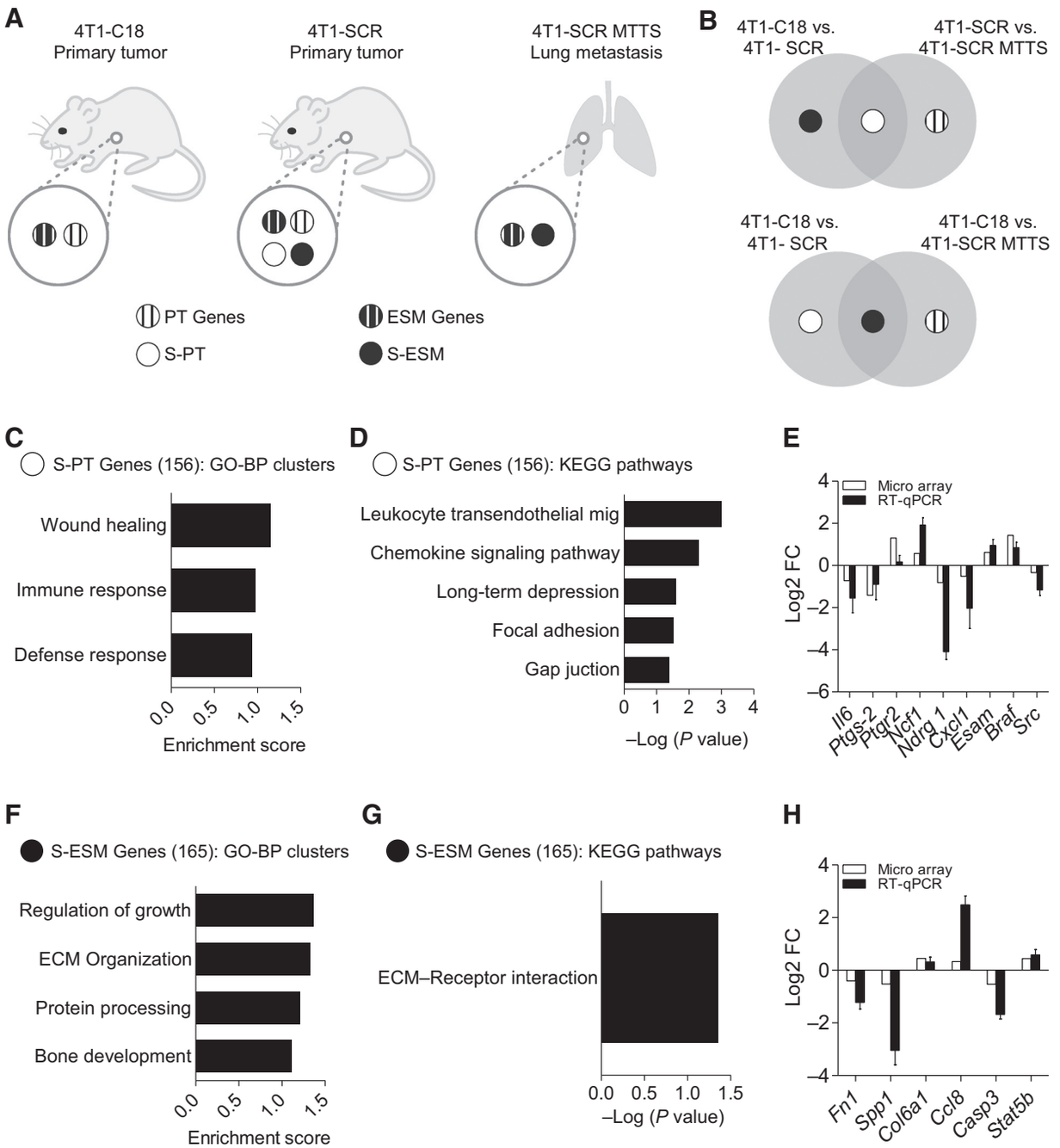

Figure 3.

SPARC-dependent genes associated with primary tumor growth and lung metastasis establishment. **A,** Model depicting the coexistence in primary tumors of two groups of genes involved in primary tumor growth (PT) and early-stage of metastasis (ESM)t that might be or not under SPARC (S) regulation (see the text for details). **B,** Top, Venn's diagram showing that S-PT genes are those differentially expressed between 4T1-SCR versus 4T1-C18 primary tumors, shared with the genes differentially expressed between 4T1-SCR primary tumor versus 4T1-SCR MTTS. Bottom, Venn's diagram showing that S-ESM genes are those differentially expressed between 4T1-SCR versus 4T1-C18 primary tumors, shared with the genes differentially expressed between 4T1-C18 primary tumors versus 4T1-SCR MTTS. **C** and **D,** Clusters of GO Biological Process (BP) and KEGG pathways enrichment analysis of S-PT genes. **E,** RT-qPCR validation of six S-PT genes identified in the microarray. **F** and **G,** Clusters of BP and KEGG pathways enrichment analysis of S-ESM genes. **H,** RT-qPCR validation of six S-ESM genes identified in the microarray. **E** and **H,** data of RT-qPCR are presented as mean ± SEM ($n = 3$). See also Supplementary Fig. S5.

Published OnlineFirst December 28, 2016; DOI: 10.1158/1541-7786.MCR-16-0243-T

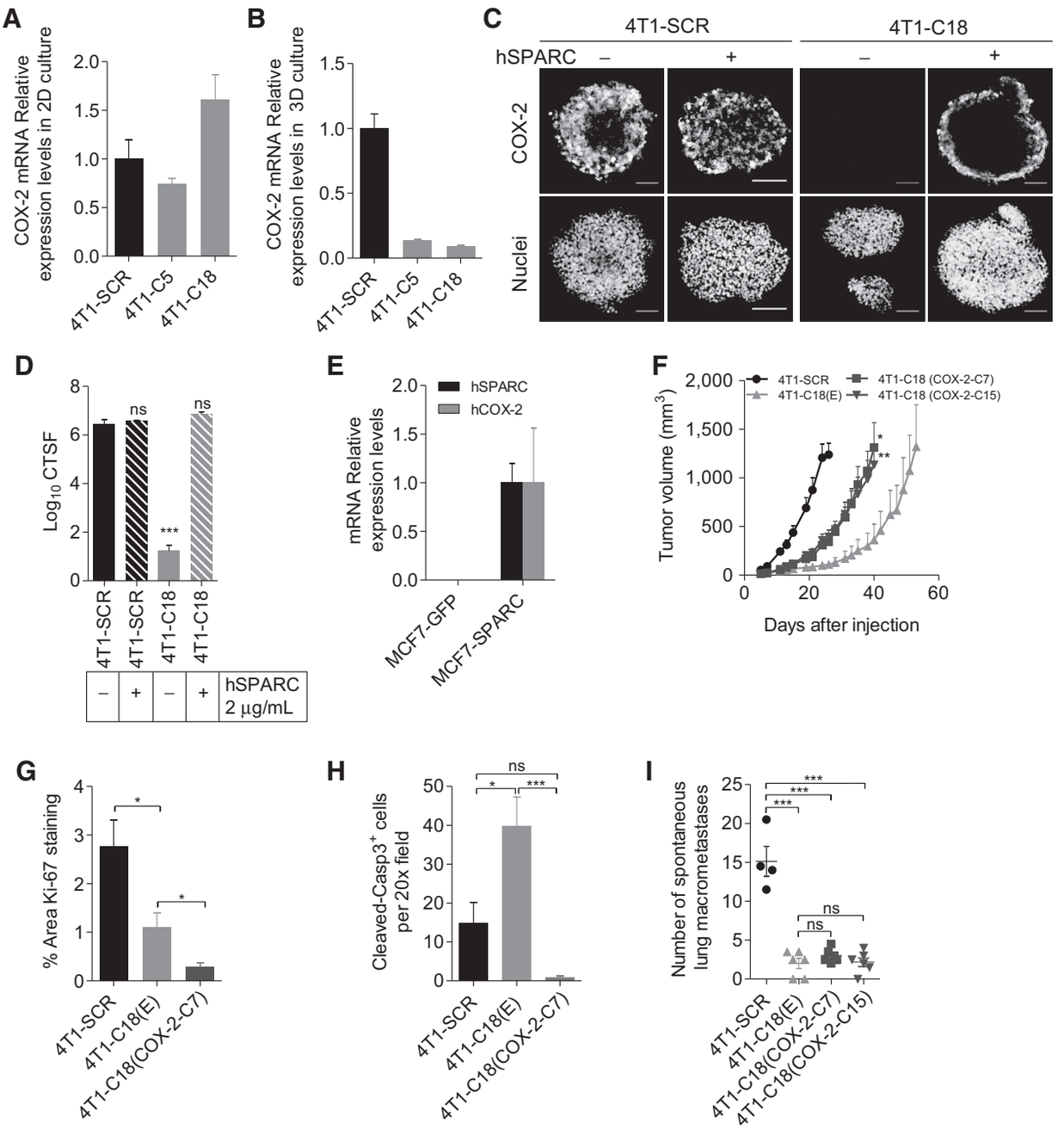

Figure 4.

SPARC-driven COX-2 expression affects primary tumor growth. **A,** RT-qPCR of COX-2 mRNA levels in cells growing as monolayer. **B,** RT-qPCR of COX-2 mRNA levels in cells' spheroids. **C,** COX-2 immunofluorescence in spheroids sections. Spheroids were grown in the presence of 2 µg/mL human purified SPARC (+) or vehicle (−) and fixed after 72 hours. Scale bars, 100 µm. **D,** Quantification of COX-2–specific fluorescence in the experiment depicted in **C**. Data are presented as mean ± SEM and are representative of three experiments. ***, $P < 0.001$, ns not significant, one-way ANOVA, and Bonferroni multiple comparisons test. **E,** RT-qPCR of SPARC and COX-2 mRNA levels in spheroids of MCF7 cells transduced with a lentivirus expressing GFP or hSPARC cDNA (MCF7-GFP and MCF7-SPARC respectively). **F,** *In vivo* growth of 4T1-SCR, 4T1-C18(E), 4T1-C18 (COX2-C7), and 4T1-C18 (COX2-C15) tumors in BALB/c mice ($n = 9$–13 mice per group). **G,** Quantification of Ki-67–positive area in tumor sections obtained at the end of the experiment depicted in **F** ($n = 3$). **H,** Quantification of cleaved caspase-3 positive cells in tumor sections at the end of the experiment depicted in **F**. **I,** Number of macroscopic foci in the lungs. Data were obtained when primary tumors reached a size of 1 cm^3 ($n = 4$–6). Data are representative of three experiments. *** $P < 0.001$; ** $P < 0.01$; *, $P < 0.05$, ns not significant, one-way ANOVA and Bonferroni multiple comparisons test. See also Supplementary Fig. S6.

Published OnlineFirst December 28, 2016; DOI: 10.1158/1541-7786.MCR-16-0243-T

COX-2 levels (Fig. 4E) confirming that COX-2 expression is under SPARC control.

The enforced expression of COX-2 in SPARC-deficient cells (Supplementary Fig. S6A) restored only partially their capacity to grow as a primary tumor (Fig. 4F). The partial restoration in tumor growth occurred despite a reduced staining in Ki67-positive cells (Fig. 4G; Supplementary Fig. S6B). Besides, these cells showed reduced *in vivo* apoptosis compared with control and SPARC-deficient tumors (Fig. 4H'; Supplementary Fig. S6C and S6D), suggesting that reduced *in vivo* apoptosis is associated with the partial restoration of tumor growth in COX-2–expressing SPARC-deficient cells. Most remarkable was the evidence that SPARC-deficient cells overexpressing COX-2 were unable to establish pulmonary metastases (Fig. 4I; Supplementary Fig. S6E), not even after intravenous administration (data not shown). These data suggest that COX-2 is not involved in SPARC-driven capacity of tumor cells to metastasize in the lungs.

SPARC modulates MDSC expansion through COX-2

Current evidence indicates that 4T1 tumors support its outgrowth in BALB/c mice by inducing a strong immunosuppressive state with systemic accumulation of MDSCS (33, 34) mainly due to tumor expression of COX-2 (35). To assess whether SPARC induces immunosuppression, we compare MDSCs ($CD11b^+Gr\text{-}1^+$) levels in control and SPARC-deficient tumor-bearing mice. We observed a systemic reduction in the percentage of MDSC in spleens ($6.9\% \pm 3.2\%$ vs. $25.3 \pm 2.0\%$; $P < 0.001$; Fig. 5A and B), lungs ($0.7\% \pm 0.2\%$ vs. $6.2\% \pm 0.9\%$; $P < 0.001$; Fig. 5C and D), and bone marrow ($48.0\% \pm 6.4\%$ vs. $62.1\% \pm 5.3\%$; $P > 0.05$; Fig. 5E and F), in mice bearing 4T1-C18 tumors compared with mice bearing 4T1-SCR tumors. Interestingly, enforced expression of COX-2 in SPARC-deficient 4T1-C18 cells restored the expansion of $CD11b^+Gr\text{-}1^+$ cells demonstrating that the SPARC-driven MDSC expansion is mediated by COX-2 (Fig. 5G). The reduced systemic levels of MDSCs was associated with an increased infiltration of $CD4^+$ and $CD8^+$ cells in SPARC-deficient primary tumors (Fig. 5H and I). Depletion of both $CD4^+$ and $CD8^+$ T cells partially restored 4T1-C18 primary tumor growth in BALB/c mice (Fig. 5J) but had no effect on the establishment of metastatic foci (Fig. 5K). Overall, these results suggest that SPARC drives a COX-2–mediated MDSC expansion to evade immune surveillance affecting only primary tumor growth, but not metastatic dissemination to the lungs.

SPARC knockdown impairs lung foci colonization through the modulation of cell–ECM interaction

Gene enrichment analyses indicated that S-ESM genes are associated with cell–ECM interaction. SPARC has been widely associated with the modulation of cell–ECM interactions (36). As mentioned before, SPARC-deficient 4T1-C18 cells exhibited a reduced capacity to enter into circulation compared with control 4T1-SCR cells (Fig. 6A) that was coincidental with the reduced *in vitro* invasiveness of SPARC-deficient cell clones (Fig. 6B; Supplementary Fig. S7A). SPARC-deficient cell clones injected intravenously generated less than five experimental metastatic foci per lung compared with more than 100 foci generated by control cells (Fig. 6C). This was confirmed by *in vivo* infrared tracking of DiR-prelabeled cells showing that 4T1-C18 cells were unable to colonize the lungs, suggesting an active role of SPARC in the initial establishment of the metastatic niche in the lung (Fig. 6D and E). Consistent with this, SPARC-deficient 4T1-C18 cells displayed a reduced ability to adhere to a fibronectin matrix (Fig. 6F). Further analysis of the S-ESM genes showed that the expression of fibronectin 1 was downregulated in SPARC-deficient tumors compared with both the 4T1-SCR tumors and the 4T1-SCR metastases (Fig. 3G; Supplementary Table S10). Overall, these data indicate that SPARC regulation of cell–ECM interaction is essential for lung colonization.

The S-PT and S-ESM molecular signatures predict outcome of patients with HER2-enriched breast tumors

We next asked whether the orthologs of SPARC-regulated genes in 4T1 primary tumors might play a role in the clinical outcome of human breast cancer patients. We used GOBO tool (30) to stratified samples into two groups based on hS-PT or hS-ESM gene expression quantiles and performed Kaplan–Meier analysis. Interestingly, we found significant differences in DMFS between two groups of worse and better outcome in all breast cancer patients (Fig. 7A and C) and in HER2-enriched subtype using both the hS-PT and hS-ESM gene sets (Fig. 7B and D; and Supplementary Fig. S8).

Discussion

Tumor heterogeneity is a hallmark of solid adenocarcinomas including human breast cancer. Most studies have shown that paired primary tumor and asynchronous metastasis are clonally related (37); the frequency of certain mutations associated to specific primary tumor cell clones prevails in the invasive and metastatic carcinoma indicating that a signature of metastasis is present in the primary tumor (2, 38). On the basis of these findings, we decided to knock down SPARC expression looking for changes that might affect breast cancer progression in an immunocompetent model.

Our study showed that SPARC produced by breast cancer epithelial cells plays a fundamental role in primary tumor growth and lung metastatic colonization in immunocompetent mammary tumor models. This comprehensive study, which involved knocking down SPARC expression in malignant epithelial cells followed by transcriptomic analysis, demonstrates that SPARC drives primary tumor growth and metastasis through independent, but not mutually exclusive, mechanisms. SPARC promotes primary tumor growth through the regulation of cell cycling and viability as well as the induction of an immunosuppressive state. The role of SPARC in lung metastasis is mainly associated with the stimulation of the ability of the malignant cells to detach from the primary tumor, invade, and enhance its adhesion in the lung parenchyma. The relevance of SPARC in human breast cancer progression is here highlighted by the predictive capacity of the molecular signatures associated with SPARC on the outcome of patients with the HER2-enriched breast cancer–aggressive subtype.

Both the *in vitro* and the *in vivo* transcriptome analyses confirmed that SPARC controls cell cycling. SPARC silencing induced a p53-independent delay in the cell-cycle progression of 4T1 cells (Supplementary Fig. S4F), with extended G_1 and G_2 phases; this effect was associated with the induction of *Wee1* and *Cdc27* expression as well as the downregulation of Cyclin B1 and B2 (Supplementary Table S4). In coincidence, SPARC-deficient tumors exhibited reduced levels of Ki67-positive cells coupled

Published OnlineFirst December 28, 2016; DOI: 10.1158/1541-7786.MCR-16-0243-T

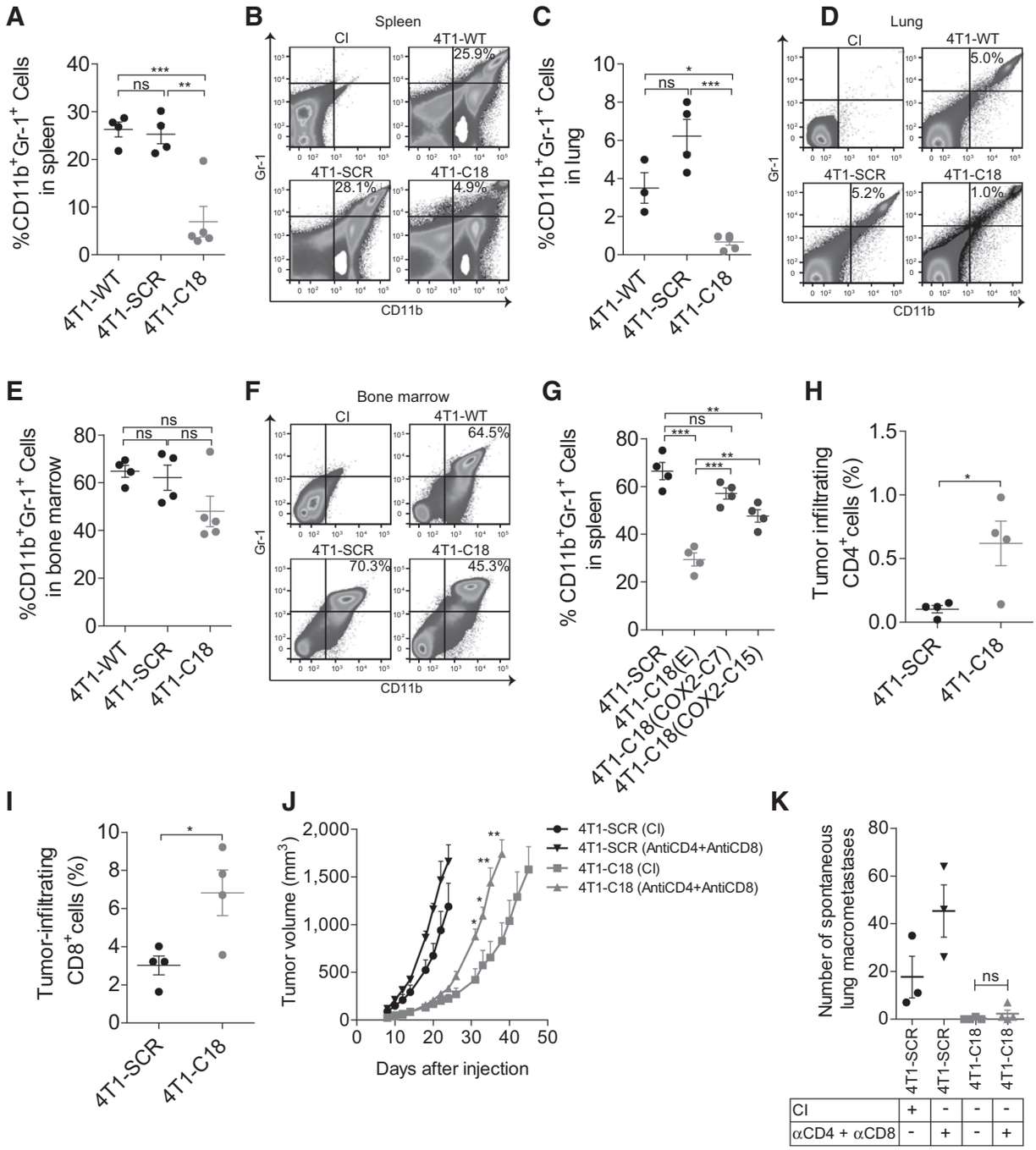

Figure 5.

SPARC drives MDSCs expansion through COX-2. Percentage of spleen (**A**), lung (**C**), and bone marrow (**E**) $CD11b^+Gr\text{-}1^+$ cells in mice harboring different tumor types ($n = 4$ mice per group). **B**, **D**, and **F,** Representative dot plots of data depicted in **A**, **C**, and **E**, respectively. Numbers within dot plots correspond to the percentages of cells in each marked region. **G,** Percentage of $CD11b^+Gr\text{-}1^+$ cells in spleen of mice challenged with different tumor types ($n = 4$ mice per group). **H** and **I,** Percentage of intratumoral $CD4^+$ and $CD8^+$ cells in mice harboring the different tumor types ($n = 4$ mice per group). **J,***In vivo* tumor growth of 4T1-SCR or 4T1-C18 cells. Mice were treated with an intraperitoneal injection of the indicated mAbs. Control mice received the equivalent amounts of normal rat IgG at the same days (Cl; $n = 4$ mice per group). **B**, **D**, and **F–J,** Data are presented as mean ± SEM and are representative of three experiments. *, $P < 0.05$; **, $P < 0.01$; ***, $P < 0.001$; ns, not significant, one-way ANOVA, and Bonferroni multiple comparisons test. **K,** Number of lung macroscopic foci of 4T1-SCR and 4T1-C18 tumor-bearing mice. Tumor-bearing mice were treated with the indicated mAbs. Data are presented as mean ± SEM. ns, not significant, unpaired *t* test, with Welch correction.

Published OnlineFirst December 28, 2016; DOI: 10.1158/1541-7786.MCR-16-0243-T

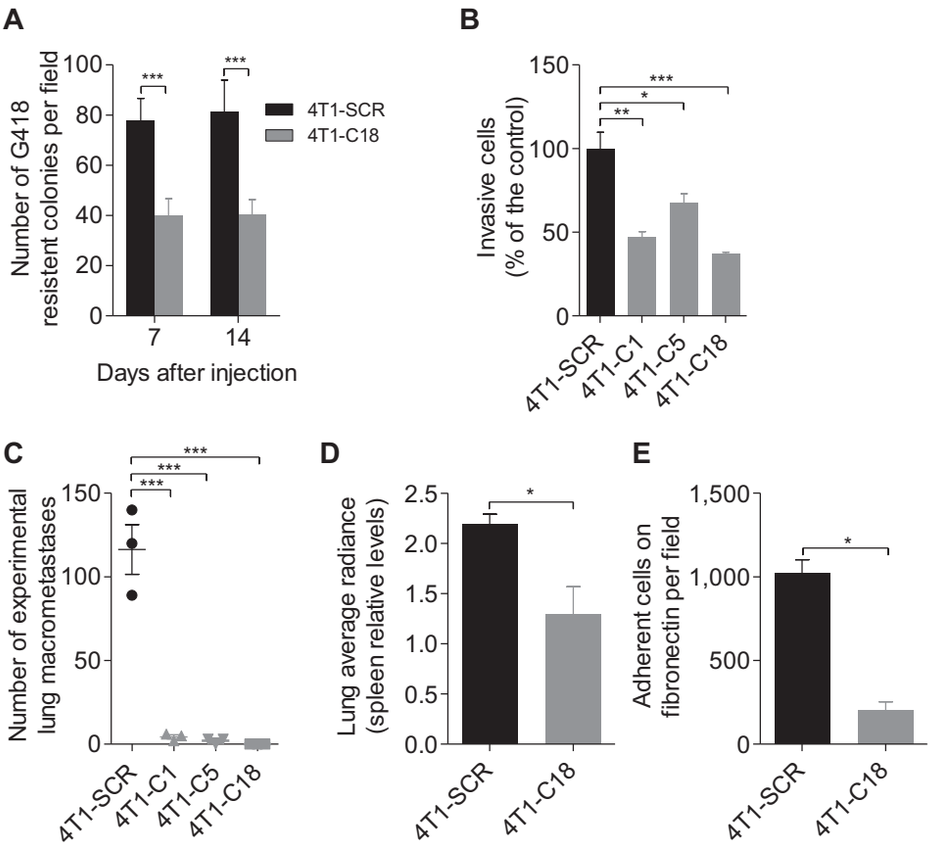

Figure 6.
SPARC modulates the early stages of metastatic dissemination and establishment of lung foci. **A,** Amount of circulating tumor cells. **B,** *In vitro* invasion assays. **C,** Number of macroscopic metastatic foci after tail vein injection of the tumors indicated in each panel ($n = 3$ mice per group). **D,** Quantification of fluorescence intensity in lungs of naïve mice five hours after intravenous injection of DiR-stained cells. The average radiance of lungs was relativized to the average radiance of spleen ($n = 3$ mice per group). **E,** Adhesion assays on fibronectin showing cells per field after 20 minutes plating. Data are the mean ± SEM of three experiments. ***, $P < 0.001$; **, $P < 0.01$; *, $P < 0.05$, one-way ANOVA, and Bonferroni multiple comparisons test. See also Supplementary Fig. S7.

with increased levels of apoptotic cells; this balance between cell cycling and cell viability could explain at least in part the reduced capacity of SPARC-deficient cells to grow into a primary tumor. The current data are consistent with previous findings showing that SPARC depletion in melanoma cells promoted G_2–M cell-cycle arrest and downregulation of cdk1 and Cyclin B1 expression, through a p53/p21Cip1/Waf1–dependent mechanism (39, 40). Notably, the overexpression of COX-2 completely restored the viability of SPARC-deficient cells. However, these changes in cell viability had only a partial effect on the capacity of SPARC-deficient cells to grow as a primary tumor indicating that additional mechanisms were implicated in this process.

COX-2 is a marker for highly aggressive human breast cancer (41) and promotes tumor progression in experimental models by reducing cancer cell apoptosis and inducing immune escape (35, 42). We observed the downregulation of COX-2 expression in SPARC-deficient tumors and further confirmed that COX-2 expression levels are under SPARC control. Interestingly, reexpression of COX-2 in SPARC-deficient cells partially restored primary tumor growth capacity but had no effect on lung metastasis establishment, not even when experimental metastases were induced by direct injection through the tail vein. These experiments confirmed that COX-2 belongs to the S-PT genes group. Interestingly, COX-2 was shown to play a role as a downstream mediator of SPARC effect on MDSC expansion. MDSC render the tumor microenvironment less permissive to the functionality of the T cells (43). In close correlation with a more permissive microenvironment, we observed an increased infiltration of $CD4^+$ and $CD8^+$ T cells in SPARC-deficient tumors. However, depletion experiments revealed that T cells were involved only in restricting primary tumor growth with no remarkable role in SPARC-driven lung metastasis establishment. Previous data in immunocompromised mice models suggested that SPARC produced by malignant cells might affect the innate immune response against human xenografted tumors (19, 20, 44). This is the first work showing that both the innate and the adaptive immune response are under the control of SPARC produced by the malignant cells. This immune response, mediated in part by COX-2, played a significant role on the primary tumor growth but not on the establishment of metastatic foci. During the time this work was under revision, an article was published showing that the overexpression of SPARC in HER-2–induced SPARC-negative breast cancer cells induced an epithelial–mesenchymal transition accompanied by a COX-2–mediated expansion of MDSC (45). This study confirms our conclusions in terms of COX-2–mediated expansion of MDSC although we were unable to see changes in the expression levels of genes associated with EMT in our model (data not shown). Other matricellular proteins, such as galectin-1 and osteopontin (whose expression is regulated by SPARC), also promote breast tumor evasion from innate and adaptive immune response, suggesting the existence of a shared function of this pleiotropic family of proteins in tumor progression (46, 47).

Independently from the abovementioned processes, SPARC promotes metastasis by regulating cell–ECM interaction driving the disengagement of malignant cells from the primary tumor and the adherence to the lung parenchyma. Indeed, the amounts of

Published OnlineFirst December 28, 2016; DOI: 10.1158/1541-7786.MCR-16-0243-T

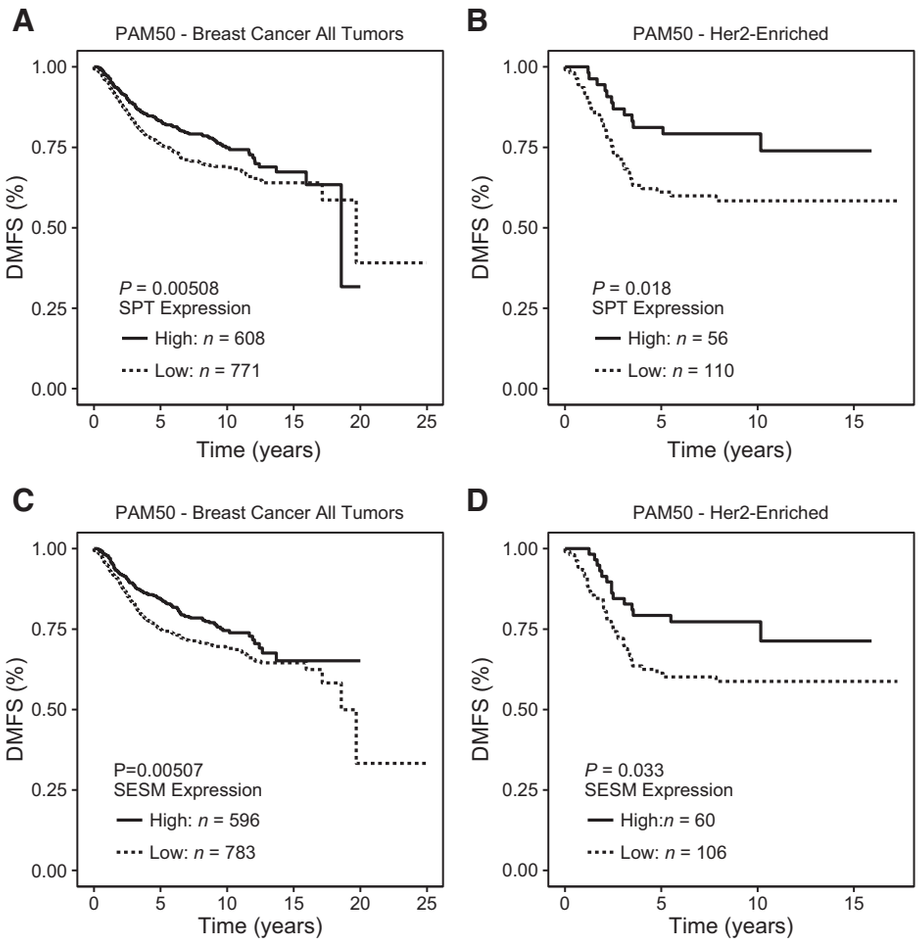

Figure 7.
Human orthologs of S-PT and S-ESM genes predict clinical outcome of HER2-enriched patients. **A** and **B,** Association between expression of hS-PT and DMFS of breast cancer patients. **A,** All patients ($n = 1,379$, high: 608, low: 771; $P < 0.01$). **B,** Patients with HER2-enriched subtype ($n = 166$, high: 56, low: 110; $P < 0.05$). **C** and **D,** Association between expression of hS-ESM and DMFS of breast cancer patients. **C,** All patients ($n = 1,379$, high: 596, low: 783; $P < 0.01$). **D,** Patients with HER2-enriched subtype ($n = 166$, high: 60, low: 106; $P < 0.05$). The analyses were performed with Gene Expression-Based Outcome for Breast Cancer Online tool. See also Supplementary Fig. S8.

circulating tumor cells decreased in SPARC-deficient tumor-bearing mice and such changes correlated with the reduced *in vitro* invasiveness of SPARC-deficient cells. Moreover, intravenously injected SPARC-deficient cells were unable to colonize the lung and establish metastatic foci, mainly because of an impairment in their ability to adhere to the lung. In the article that appeared when this manuscript was under revision, it was also suggested that MDSCs play a key role in the metastatic capabilities of mammary tumor cells (45). Although we cannot rule out the involvement of MDSCs in lung colonization, our data point to SPARC regulation of cell–ECM interaction as the driven mechanism. Consistent with the evidence that SPARC can regulate cell-to-cell and cell–ECM interaction, a recent report demonstrated that SPARC expressed by melanoma cells induced vascular permeability, extravasation, and lung metastasis through direct interaction with VCAM1 (48).

A remarkable finding in the current study was that both SPARC and SPARC-driven gene signatures predict the outcome of the HER2-enriched group of breast cancer patients. As we mentioned in the Introduction, most studies including the current one, favor the view that SPARC expression is associated with a more aggressive, less differentiated phenotype of human breast cancer. Interestingly, *in silico* studies found a clear association between high SPARC levels and poor prognosis in the HER2-enriched breast cancer subtype (11). Here, we confirmed and extended those findings by showing that not only SPARC but also downstream effectors associated with inflammatory/immune responses and cell–ECM interactions have prognostic significance in HER2-enriched breast cancer patients. Interestingly, immune response and tumor invasion, two processes regulated by SPARC in the current studies, were also associated with prognosis in $HER2^+$ breast cancer patients (49–51), suggesting a potential link between SPARC-driven effects and HER2-enriched patients' outcome.

In conclusion, the current study confirms that SPARC plays a protumorigenic and prometastatic role in breast cancer through alternative, non-exclusive mechanisms. The present data highlights the tumor-associated pathways under SPARC control and points SPARC, and its downstream effectors, as attractive targets for the design of rational therapies.

Disclosure of Potential Conflicts of Interest

No potential conflicts of interest were disclosed.

Authors' Contributions

Conception and design: L.N. Guttlein, L.G. Benedetti, V. Gottifredi, N.W. Zwirner, A.S. Llera, O.L. Podhajcer

Development of methodology: L.N. Guttlein, L.G. Benedetti, R.G. Spallanzani, S.F. Mansilla, O.L. Podhajcer

Acquisition of data (provided animals, acquired and managed patients, provided facilities, etc.): L.N. Guttlein, L.G. Benedetti, R.G. Spallanzani, S.F. Mansilla, C. Rotondaro, X.L. Raffo Iraolagoitia, E. Salvatierra

Analysis and interpretation of data (e.g., statistical analysis, biostatistics, computational analysis): L.N. Guttlein, L.G. Benedetti, C. Fresno, E.A. Fernandez
Writing, review, and/or revision of the manuscript: L.N. Guttlein, L.G. Benedetti, C. Fresno, E.A. Fernandez, V. Gottifredi, N.W. Zwirner, A.S. Llera, O.L. Podhajcer
Administrative, technical, or material support (i.e., reporting or organizing data, constructing databases): C. Rotondaro, A.I. Bravo
Study supervision: A.S. Llera, O.L. Podhajcer

Acknowledgments

The authors acknowledge the continuous support of AFULIC from Rio Cuarto, Argentina. We thank Maximiliano Neme and Leonardo Sganga for technical assistance with microscopy studies and flow cytometry studies respectively, and G. Mazzolini, F. Pitossi, and J. Mordoh for providing us with different antibodies.

Grant Support

This work was supported by AFULIC (Amigos de la Fundacion Leloir para Investigación contra el Cáncer).

The costs of publication of this article were defrayed in part by the payment of page charges. This article must therefore be hereby marked *advertisement* in accordance with 18 U.S.C. Section 1734 solely to indicate this fact.

Received July 20, 2016; revised November 25, 2016; accepted December 7, 2016; published OnlineFirst December 28, 2016.

References

1. Howlader N, Noone AM, Krapcho M, Miller D, Bishop K, Altekruse SF, et al. SEER Cancer Statistics Review, 1975–2013. Bethesda, MD: National Cancer Institute; 2016. Available from: http://seer.cancer.gov/csr/1975_2013/.
2. Ramaswamy S, Ross KN, Lander ES, Golub TR. A molecular signature of metastasis in primary solid tumors. Nat Genet 2003;33:49–54.
3. Cummings MC, Simpson PT, Reid LE, Jayanthan J, Skerman J, Song S, et al. Metastatic progression of breast cancer: insights from 50 years of autopsies. J Pathol 2014;232:23–31.
4. Minn AJ, Gupta GP, Siegel PM, Bos PD, Shu W, Giri DD, et al. Genes that mediate breast cancer metastasis to lung. Nature 2005;436:518–24.
5. Watkins G, Douglas-Jones A, Bryce R, Mansel RE, Jiang WG. Increased levels of SPARC (osteonectin) in human breast cancer tissues and its association with clinical outcomes. Prostaglandins Leukot Essent Fatty Acids 2005;72:267–72.
6. Park SY, Lee HE, Li H, Shipitsin M, Gelman R, Polyak K. Heterogeneity for stem cell-related markers according to tumor subtype and histologic stage in breast cancer. Clin Cancer Res 2010;16:876–87.
7. Witkiewicz AK, Freydin B, Chervoneva I, Potoczek M, Rizzo W, Rui H, et al. Stromal CD10 and SPARC expression in ductal carcinoma in situ (DCIS) patients predicts disease recurrence. Cancer Biol Ther 2010;10:391–6.
8. Hsiao YH, Lien HC, Hwa HL, Kuo WH, Chang KJ, Hsieh FJ. SPARC (osteonectin) in breast tumors of different histologic types and its role in the outcome of invasive ductal carcinoma. Breast J 2010;16:305–8.
9. Bergamaschi A, Tagliabue E, Sorlie T, Naume B, Triulzi T, Orlandi R, et al. Extracellular matrix signature identifies breast cancer subgroups with different clinical outcome. J Pathol 2008;214:357–67.
10. Eswaran J, Cyanam D, Mudvari P, Reddy SD, Pakala SB, Nair SS, et al. Transcriptomic landscape of breast cancers through mRNA sequencing. Sci Rep 2012;2:264.
11. Azim HA Jr, Singhal S, Ignatiadis M, Desmedt C, Fumagalli D, Veys I, et al. Association between SPARC mRNA expression, prognosis and response to neoadjuvant chemotherapy in early breast cancer: a pooled in-silico analysis. PLoS One 2013;8:e62451.
12. Helleman J, Jansen MP, Ruigrok-Ritstier K, van Staveren IL, Look MP, Meijer-van Gelder ME, et al. Association of an extracellular matrix gene cluster with breast cancer prognosis and endocrine therapy response. Clin Cancer Res 2008;14:5555–64.
13. Beck AH, Espinosa I, Gilks CB, van de Rijn M, West RB. The fibromatosis signature defines a robust stromal response in breast carcinoma. Lab Invest 2008;88:591–601.
14. Nagai MA, Gerhard R, Fregnani JH, Nonogaki S, Rierger RB, Netto MM, et al. Prognostic value of NDRG1 and SPARC protein expression in breast cancer patients. Breast Cancer Res Treat 2011;126:1–14.
15. Lien HC, Hsiao YH, Lin YS, Yao YT, Juan HF, Kuo WH, et al. Molecular signatures of metaplastic carcinoma of the breast by large-scale transcriptional profiling: identification of genes potentially related to epithelial-mesenchymal transition. Oncogene 2007;26:7859–71.
16. Briggs J, Chamboredon S, Castellazzi M, Kerry JA, Bos TJ. Transcriptional upregulation of SPARC, in response to c-Jun overexpression, contributes to increased motility and invasion of MCF7 breast cancer cells. Oncogene 2002;21:7077–91.
17. Gilles C, Bassuk JA, Pulyaeva H, Sage EH, Foidart JM, Thompson EW. SPARC/osteonectin induces matrix metalloproteinase 2 activation in human breast cancer cell lines. Cancer Res 1998;58:5529–36.
18. Koblinski JE, Kaplan-Singer BR, VanOsdol SJ, Wu M, Engbring JA, Wang S, et al. Endogenous osteonectin/SPARC/BM-40 expression inhibits MDA-MB-231 breast cancer cell metastasis. Cancer Res 2005;65:7370–7.
19. Ledda MF, Adris S, Bravo AI, Kairiyama C, Bover L, Chernajovsky Y, et al. Suppression of SPARC expression by antisense RNA abrogates the tumorigenicity of human melanoma cells. Nat Med 1997;3:171–6.
20. Alvarez MJ, Prada F, Salvatierra E, Bravo AI, Lutzky VP, Carbone C, et al. Secreted protein acidic and rich in cysteine produced by human melanoma cells modulates polymorphonuclear leukocyte recruitment and antitumor cytotoxic capacity. Cancer Res 2005;65:5123–32.
21. Sangaletti S, Stoppacciaro A, Guiducci C, Torrisi MR, Colombo MP. Leukocyte, rather than tumor-produced SPARC, determines stroma and collagen type IV deposition in mammary carcinoma. J Exp Med 2003;198:1475–85.
22. Sangaletti S, Di Carlo E, Gariboldi S, Miotti S, Cappetti B, Parenza M, et al. Macrophage-derived SPARC bridges tumor cell-extracellular matrix interactions toward metastasis. Cancer Res 2008;68:9050–9.
23. Tang J, Hu M, Lee S, Roblin R. Primer mixture enhances PCR detection of Mycoplasma/Acholeplasma contaminants in cell cultures. In Vitro Cell Dev Biol Anim 1999;35:1–3.
24. Carpenter AE, Jones TR, Lamprecht MR, Clarke C, Kang IH, Friman O, et al. CellProfiler: image analysis software for identifying and quantifying cell phenotypes. Genome Biol 2006;7:R100.
25. Schneider CA, Rasband WS, Eliceiri KW. NIH Image to ImageJ: 25 years of image analysis. Nat Methods 2012;9:671–5.
26. Adris S, Chuluyan E, Bravo A, Berenstein M, Klein S, Jasnis M, et al. Mice vaccination with interleukin 12-transduced colon cancer cells potentiates rejection of syngeneic non-organ-related tumor cells. Cancer Res 2000;60:6696–703.
27. Rubinstein N, Alvarez M, Zwirner NW, Toscano MA, Ilarregui JM, Bravo A, et al. Targeted inhibition of galectin-1 gene expression in tumor cells results in heightened T cell-mediated rejection; A potential mechanism of tumor-immune privilege. Cancer Cell 2004;5:241–51.
28. Kanehisa M, Goto S. KEGG: kyoto encyclopedia of genes and genomes. Nucleic Acids Res 2000;28:27–30.
29. Ashburner M, Ball CA, Blake JA, Botstein D, Butler H, Cherry JM, et al. Gene ontology: tool for the unification of biology. The Gene Ontology Consortium. Nat Genet 2000;25:25–9.
30. Ringner M, Fredlund E, Hakkinen J, Borg A, Staaf J. GOBO: gene expression-based outcome for breast cancer online. PLoS One 2011;6:e17911.
31. Aslakson CJ, Miller FR. Selective events in the metastatic process defined by analysis of the sequential dissemination of subpopulations of a mouse mammary tumor. Cancer Res 1992;52:1399–405.
32. Urtreger A, Ladeda V, Puricelli L, Rivelli A, Vidal M, Delustig E, et al. Modulation of fibronectin expression and proteolytic activity associated with the invasive and metastatic phenotype in two new murine mammary tumor cell lines. Int J Oncol 1997;11:489–96.
33. Chandra D, Jahangir A, Quispe-Tintaya W, Einstein MH, Gravekamp C. Myeloid-derived suppressor cells have a central role in attenuated Listeria

monocytogenes-based immunotherapy against metastatic breast cancer in young and old mice. Br J Cancer 2013;108:2281–90.
34. Spallanzani RG, Dalotto-Moreno T, Raffo Iraolagoitia XL, Ziblat A, Domaica CI, Avila DE, et al. Expansion of CD11b(+)Ly6G (+)Ly6C (int) cells driven by medroxyprogesterone acetate in mice bearing breast tumors restrains NK cell effector functions. Cancer Immunol Immunother 2013; 62:1781–95.
35. Sinha P, Clements VK, Fulton AM, Ostrand-Rosenberg S. Prostaglandin E2 promotes tumor progression by inducing myeloid-derived suppressor cells. Cancer Res 2007;67:4507–13.
36. Podhajcer OL, Benedetti LG, Girotti MR, Prada F, Salvatierra E, Llera AS. The role of the matricellular protein SPARC in the dynamic interaction between the tumor and the host. Cancer Metastasis Rev 2008;27:691–705.
37. Zardavas D, Irrthum A, Swanton C, Piccart M. Clinical management of breast cancer heterogeneity. Nat Rev Clin Oncol 2015;12:381–94.
38. Heselmeyer-Haddad K, Berroa Garcia LY, Bradley A, Ortiz-Melendez C, Lee WJ, Christensen R, et al. Single-cell genetic analysis of ductal carcinoma in situ and invasive breast cancer reveals enormous tumor heterogeneity yet conserved genomic imbalances and gain of MYC during progression. Am J Pathol 2012;181:1807–22.
39. Fenouille N, Robert G, Tichet M, Puissant A, Dufies M, Rocchi S, et al. The p53/p21Cip1/Waf1 pathway mediates the effects of SPARC on melanoma cell cycle progression. Pigment Cell Melanoma Res 2011;24:219–32.
40. Fenouille N, Puissant A, Tichet M, Zimniak G, Abbe P, Mallavialle A, et al. SPARC functions as an anti-stress factor by inactivating p53 through Akt-mediated MDM2 phosphorylation to promote melanoma cell survival. Oncogene 2011;30:4887–900.
41. Ristimaki A, Sivula A, Lundin J, Lundin M, Salminen T, Haglund C, et al. Prognostic significance of elevated cyclooxygenase-2 expression in breast cancer. Cancer Res 2002;62:632–5.
42. Basu GD, Pathangey LB, Tinder TL, Lagioia M, Gendler SJ, Mukherjee P. Cyclooxygenase-2 inhibitor induces apoptosis in breast cancer cells in an in vivo model of spontaneous metastatic breast cancer. Mol Cancer Res 2004;2:632–42.
43. Gabrilovich DI, Ostrand-Rosenberg S, Bronte V. Coordinated regulation of myeloid cells by tumours. Nat Rev Immunol 2012;12: 253–68.
44. Prada F, Benedetti LG, Bravo AI, Alvarez MJ, Carbone C, Podhajcer OL. SPARC endogenous level, rather than fibroblast-produced SPARC or stroma reorganization induced by SPARC, is responsible for melanoma cell growth. J Invest Dermatol 2007;127:2618–28.
45. Sangaletti S, Tripodo C, Santangelo A, Castioni N, Portararo P, Gulino A, et al. Mesenchymal transition of high-grade breast carcinomas depends on extracellular matrix control of myeloid suppressor cell activity. Cell Rep 2016;17:233–48.
46. Dalotto-Moreno T, Croci DO, Cerliani JP, Martinez-Allo VC, Dergan-Dylon S, Mendez-Huergo SP, et al. Targeting galectin-1 overcomes breast cancer-associated immunosuppression and prevents metastatic disease. Cancer Res 2013;73:1107–17.
47. Sangaletti S, Tripodo C, Sandri S, Torselli I, Vitali C, Ratti C, et al. Osteopontin shapes immunosuppression in the metastatic niche. Cancer Res 2014;74:4706–19.
48. Tichet M, Prod'Homme V, Fenouille N, Ambrosetti D, Mallavialle A, Cerezo M, et al. Tumour-derived SPARC drives vascular permeability and extravasation through endothelial VCAM1 signalling to promote metastasis. Nat Commun 2015;6:6993.
49. Staaf J, Ringner M, Vallon-Christersson J, Jonsson G, Bendahl PO, Holm K, et al. Identification of subtypes in human epidermal growth factor receptor 2–positive breast cancer reveals a gene signature prognostic of outcome. J Clin Oncol 2010;28:1813–20.
50. Desmedt C, Haibe-Kains B, Wirapati P, Buyse M, Larsimont D, Bontempi G, et al. Biological processes associated with breast cancer clinical outcome depend on the molecular subtypes. Clin Cancer Res 2008;14: 5158–65.
51. Alexe G, Dalgin GS, Scanfeld D, Tamayo P, Mesirov JP, DeLisi C, et al. High expression of lymphocyte-associated genes in node-negative HER2+ breast cancers correlates with lower recurrence rates. Cancer Res 2007;67:10669–76.

Published OnlineFirst December 28, 2016; DOI: 10.1158/1541-7786.MCR-16-0243-T

Molecular Cancer Research

Predictive Outcomes for HER2-enriched Cancer Using Growth and Metastasis Signatures Driven By SPARC

Leandro N. Güttlein, Lorena G. Benedetti, Cristóbal Fresno, et al.

Mol Cancer Res 2017;15:304-316. Published OnlineFirst December 28, 2016.